

# Searching for Planets in the Hyades III: The Quest for Short-Period Planets <sup>1, 2</sup>

Diane B. Paulson<sup>3</sup>

*Department of Astronomy, University of Texas, Austin, TX 78712*

`apodis@astro.as.utexas.edu`

Steven H. Saar

*Center for Astrophysics, 60 Garden Street, Cambridge, MA 02138*

`ssaar@cfa.harvard.edu`

William D. Cochran

*McDonald Observatory, University of Texas, Austin, TX 78712*

`wdc@astro.as.utexas.edu`

and

Gregory W. Henry<sup>4</sup>

*Center of Excellence in Information Systems, Tennessee State University, Nashville, TN 37203*

`henry@schwab.tsuniv.edu`

## ABSTRACT

We have been using the Keck I High Resolution Spectrograph (HIRES) to search for planetary companions in the Hyades cluster. We selected four stars from this sample which showed significant radial velocity variability on short timescales to search for short-period planetary companions. The radial velocities of these four stars were monitored regularly with the Hobby Eberly Telescope (HET) for approximately two months, while sparse data were also taken over  $\sim 4$  months: we also obtained near-simultaneous photometric observations with one of the automatic photoelectric telescopes at Fairborn Observatory. For three of the stars, we detect photometric variability with the same period present in the radial velocity ( $v_r$ ) measurements, compatible with the expected rotation rates for Hyades members. The fourth star continues to show  $v_r$  variations and

---

<sup>3</sup>current address: Department of Astronomy, University of Michigan, 830 Dennison, Ann Arbor, MI 48109

<sup>4</sup>Also Senior Research Associate, Department of Physics and Astronomy, Vanderbilt University, Nashville, TN 37235

minimal photometric variability but with no significant periodicity. This study shows that for the three stars with periodic behavior, a significant portion of the  $v_r$  fluctuations are likely due primarily to magnetic activity modulated by stellar rotation rather than planetary companions. Using simple models for the  $v_r$  perturbations arising from spot and plage, we demonstrate that *both* are likely to contribute to the observed  $v_r$  variations. Thus, simultaneous monitoring of photometric (photospheric) and spectroscopic (chromospheric) variations is essential for identifying the cause of Doppler shifted absorption lines in more active stars.

*Subject headings:* clusters: open (Hyades) — stars: spots — stars: planetary systems — techniques: radial velocities — techniques: photometric — stars: activity

## 1. Introduction

It is well known that starspots will cause shifts in line profile shapes (cf. Vogt et al. 1987), which will cause apparent Doppler shifts of the lines. Saar & Donahue (1997) modeled the expected  $v_r$  variability due to the rotational modulation of spots. Hatzes (1999) and Hatzes (2002) make similar calculations and obtain the same results as Saar & Donahue (1997). Recently, observational data to support this has been published. Queloz et al. (2001) found HD 166435 to have a large velocity amplitude, but it turned out also to show sinusoidal photometric amplitude in Strömgren  $y$  with the same period. In addition, the Calcium HK index varied smoothly on the same timescale. This indicated the  $v_r$  variations were most likely due to stellar activity rather than a planetary companion. Henry et al. (2002) showed starspots to be the cause of the line shifts in HD 192263 and GWH and P. Butler see the same thing in HD 19632 (private communication, 2002). Additionally, Saar et al. (1998) and Santos et al. (2000) confirm the models presented by Saar & Donahue (1997).

The amplitude of  $v_r$  caused by plage regions is also beginning to be modeled (Saar 2003). He finds that this can be several tens of  $\text{m s}^{-1}$ . Therefore, it is important that one monitor all aspects of stellar activity when searching for planets, particularly around active stars. Here, we investigate the implications of the rotational modulation of stellar activity on our search for short-period planets in the Hyades.

---

<sup>1</sup>Some data were obtained with the HET. The Hobby-Eberly Telescope is operated by McDonald Observatory on behalf of The University of Texas at Austin, the Pennsylvania State University, Stanford University, Ludwig-Maximilians-Universität München, and Georg-August-Universität Göttingen.

<sup>2</sup>Additional data presented herein were obtained at the W.M. Keck Observatory, which is operated as a scientific partnership among the California Institute of Technology, the University of California and the National Aeronautics and Space Administration. The Observatory was made possible by the generous financial support of the W.M. Keck Foundation.

## 2. Observations and Analysis

### 2.1. Sample

The motivations for the Keck Hyades survey are discussed by Cochran et al. (2002). With a sample of 98 stars, with  $[\text{Fe}/\text{H}]=0.13$  (Paulson et al. 2003), we might expect a small number of short-period planets similar to 51 Peg (Mayor & Queloz 1995). From our Keck Hyades sample, we chose four stars for follow-up observations with the HET’s High Resolution Spectrograph (HRS) in search of short-period planetary companions. The targets were chosen from a group of stars which showed significant  $v_r$  rms on short timescales. Only four were observed at this time due to HET scheduling constraints. The image quality of the telescope was being corrected during this time, and though this did not affect the quality of the observations, it placed a magnitude limit on the stars which could be observed. The observed targets are listed in Table 1.

### 2.2. $v_r$ measurements

The  $v_r$  observations from the Keck High Resolution Echelle Spectrograph (HIRES) are described in full in Cochran et al. (2002). We began regular observations of these four stars from late-December 2001 to Mid-February 2002 (and a few observations of each star taken sporadically during the fall of 2001) with the HRS at the HET (Tull 1998; Cochran et al. 2003). We used the 3” optical fiber feed to the HRS with resolving power  $R=60,000$ . We set the 316 g/mm cross disperser to central wavelength 5938Å. This includes almost the entire  $I_2$  region ( $\approx 5000 - 6200\text{\AA}$ ;  $I_2$  is used as the velocity metric), on one of the CCD chips. Any other configuration would result in spreading the  $I_2$  region over both CCD chips and losing some  $I_2$  information in the gap between CCDs. We manufactured the  $I_2$  gas absorption cell for use in the HRS at the University of Texas, and during these observations, it was run at 60°C.

Each exposure was restricted to 15 minutes in length to reduce velocity smearing due to the Earth’s rotation. This limited the signal-to-noise ratio (S/N), but was necessary to obtain high  $v_r$  precision (see Paulson et al. 2002). The S/N varied greatly from exposure to exposure due to seeing variations, but all observations had  $S/N \gtrsim 200$  per pixel. The CCD images were reduced and extracted using standard IRAF<sup>5</sup> packages. We use a program called RADIAL (developed at the University of Texas (UT) and McDonald Observatory) to measure precise radial velocities. This program was adapted for use with data from all of the planet search programs affiliated with UT. Brief discussions of the program may be found in Cochran et al. (1997) and Hatzes et al. (2000). The typical velocity precision for observations with the HET HRS is 4-6  $\text{m s}^{-1}$  (Cochran et al. 2003). The  $K$  amplitudes are listed in Table 1. The  $K$  amplitude for HD 26756, which is not found

---

<sup>5</sup>IRAF is distributed by the National Optical Astronomy Observatories, which are operated by the Association of Universities for Research in Astronomy, Inc., under cooperative agreement with the National Science Foundation.

to have significant periodicity, is just defined as one half of the peak-to-peak variation of the  $v_r$ . The  $v_r$  data are listed in Table 2.

### 2.3. Photometric measurements

Between 11 and 14 nightly photometric observations of each of the four stars were acquired in 2002 February and March with the T12 0.8 m automatic photoelectric telescope (APT) at Fairborn Observatory in the Patagonia Mountains of southern Arizona<sup>6</sup>. The T12 APT measures the difference in brightness between a program star and nearby comparison stars in the Strömgren  $b$  and  $y$  passbands. The observing procedures and data reduction techniques employed with this APT are identical to those for the T8 0.8 m APT described in Henry (1999). The resulting Strömgren  $b$  and  $y$  differential magnitudes were corrected for differential extinction with nightly extinction coefficients and transformed to the Strömgren system with yearly mean transformation coefficients. The external precision of the differential magnitudes, defined as the standard deviation of a single differential magnitude from the seasonal mean of the differential magnitudes, is typically around 0.0012 mag for this telescope, as determined from observations of pairs of constant stars. Our primary comparison stars for were HD 26737 (for HD 26736), HD 27561 (for HD 26756 and HD 26767), and HD 18579 (for HIP 13806); all three comparison stars are constant to  $\sim 0.003$  mag or better as determined by intercomparison with additional comparison stars. The resulting range in the differential  $y$  magnitudes ( $\Delta y$ ) of our four program stars are given in Table 1. Photometric data are listed in Table 3.

## 3. Results

### 3.1. $P_{\text{rot}}$

We are able to determine the rotational period ( $P_{\text{rot}}$ ) for these stars from both sets of observations-  $v_r$  and  $\Delta y$ , independently. We used the method of Horne & Baliunas (1986) for period determination, and all results are listed in Table 1. We independently determined periods from the photometric data using the procedure outlined in Henry et al. (2001), and these periods are as follows: HIP 13806-  $9.57 \pm 0.18$  d, HD 26736-  $8.48 \pm 0.35$  d, HD 26767-  $8.69 \pm 0.13$  d. These agree with the periods determined by the method of Horne & Baliunas (listed in Table 1). HD 26736, HD 26767 and HIP 13806 all show relatively significant periods in the period analysis, with false alarm probabilities (FAPs) of  $\lesssim 15\%$  (also calculated by the method described in Horne & Baliunas).  $P_{\text{rot}}$  is also consistent between spectroscopic and photometric data assuring us that the periods derived in  $v_r$  are due to rotational modulation of stellar activity. We chose to use  $P_{\text{rot}}$  determined from  $v_r$  to show the phase plots in Figure 1 since there were more data available. We could, equally as

---

<sup>6</sup>Further information about Fairborn Observatory can be found at <http://www.fairobs.org/>.

well, have chosen to phase the plots according to  $P_{\text{rot}}$  as derived from the photometry. Zero phase was chosen to be at photometric maximum, which roughly corresponds to the time at which the  $v_r$  curve crosses from “blue” to “red”. This is done so because photometric maximum is an easily understandable physical event, thus “grounding” the phase plot. The associated  $v_r$  plots are only the results of the active regions (photometric variations).

We searched the Hipparcos Epoch Photometry (ESA) of each of these stars for periodicity. The period finding algorithm of Horne & Baliunas was again used to search for periodicity in the Hipparcos data set. When Queloz et al. (2001) studied HD 166435, they noticed that by taking small sections of their data in time, they were able to recover  $P_{\text{rot}}$ . However, when taking the entire data set, they saw no obvious signature of  $P_{\text{rot}}$ . This was an effect of phase shifts as the spots migrated either in longitude with stellar differential rotation or in latitude *or* appeared or disappeared asymmetrically. HD 26736 and HD 26767 appear to behave like HD 166435 in that the full photometric data set from Hipparcos shows no obvious periodicity. This is also true for the  $v_r$  data sets of these stars observed from Keck, although weak signals may be present for these two stars. However, the  $P_{\text{rot}}$  is recovered when taking small intervals of Keck  $v_r$  data in time for these two program stars. The case of HIP 13806 is different; we found a strong period at 9.60 days (FAP of 0.02%) in the full Hipparcos data set. The periodogram peak is sufficiently wide that it encompasses  $P_{\text{rot}}$  derived from both  $v_r$  and  $\Delta y$ . Thus,  $P_{\text{rot}}$  is somewhat poorly defined from the Hipparcos observations alone. The phase curve for the HIP 13806 Hipparcos data with a 9.42 day period is shown in Figure 2. HIP 13806 is unusual in that the same period seems to be more or less coherent, though quite noisy, over the  $\sim 2.5$  year time frame of the Hipparcos observations. HIP 13806 is also notable in that it is one of few dwarf stars which show this long term stability of active regions. Toner & Gray (1988) also observed the G8 dwarf star  $\xi$  Boo A show a coherent period over the course of four observing seasons. Certainly, this activity is unusually stable.

### 3.2. Determination of $v \sin i$ and $i$

We determined the projected stellar rotational velocity ( $v \sin i$ ) for each of these stars using the radial velocity “template” spectra (observed without the I<sub>2</sub> cell in place) obtained during the Keck observing runs. Using the newest version of the LTE line analysis code MOOG (Sneden 1973), we first derived stellar parameters<sup>7</sup>- effective temperature ( $T_{\text{eff}}$ ), surface gravity ( $\log g$ ), microturbulence ( $\xi$ ) and metallicity ([Fe/H]) for these four stars with interpolated<sup>8</sup> atmosphere models based on the 1995 version of ATLAS9 code (Castelli et al. 1997). We used no convective overshoot in the model atmospheres. We measured equivalent widths of about 20 unblended Fe

---

<sup>7</sup>A detailed analysis of the determination of stellar parameters and abundances is provided in Paulson et al. (2003). A shortened description is provided here.

<sup>8</sup>Interpolation software was kindly supplied by McWilliam (1995, private communication) and updated by Ivans (2002, private communication).

I lines and 10 unblended Fe II lines for each star in the region 4490 to 6175Å (linelist provided in Paulson et al. 2003). In a self-consistent manner,  $gf$  values for each line were derived from the Kurucz solar atlas (Kurucz et al. 1984) and confirmed with a solar spectrum taken through HIRES. The stellar parameters derived are listed in Table 4. The average  $[\text{Fe}/\text{H}]$  values listed are relative to solar ( $\log \epsilon(\text{Fe}/\text{H})_{\odot} = 7.52$ , Sneden et al. (1991)). Using these parameters, we then synthesized a spectral region with 5 Fe I lines in the region 6150 - 6180Å. In order to determine  $v \sin i$ , we compute a disk intensity profile and then convolve that with a broadening function. This broadening function contains not only  $v \sin i$ , but also a macroturbulent velocity and an instrumental broadening. We also incorporate into it a limb darkening coefficient. We used a Gaussian profile to fit the lines of the thorium-argon (ThAr) lamp. We found a FWHM of 0.09Å defines the instrumental broadening for this spectral region. The FWHM varies from 0.0918 to 0.0921Å from the redmost to the bluest lines, and the synthesis code is insensitive to this small a change. We estimated macroturbulence ( $\zeta$ ) according to Saar & Osten (1997) for active stars and using B-V from Allende Prieto & Lambert (1999). Using estimates of limb darkening from Gray (1992), were able to derive  $v \sin i$  to within about 0.7 km s<sup>-1</sup>.

We estimated stellar radii ( $R_{\star}$ ) from Gray (1992) using derived  $T_{\text{eff}}$ , although we acknowledge that the stellar radii will be somewhat increased by the higher metallicity of the Hyades. Metal enrichment increases the opacity in the convection zone. According to hydrostatic equilibrium, as opacity is increased, the change in pressure as a function of optical depth will decrease, causing a slightly larger radius. For the purposes here, an estimate of  $R_{\star}$  based on solar metallicity will suffice.

Using  $P_{\text{rot}}$  measured from this work, we were able to estimate the rotational axis inclination ( $i$ ) of each star. The  $\sin i$  values are listed in Table 4. Adopting generous errors of 0.3 days for  $P_{\text{rot}}$  and 0.05  $R_{\odot}$  for  $R_{\star}$ , and model dependent errors of 100 K for  $T_{\text{eff}}$ , 0.3 km s<sup>-1</sup> for  $\zeta$  and 0.1 km s<sup>-1</sup> for  $\xi$ , we note that the determination of  $\sin i$  is known to within 17% for HD 26736 and HD 26767 and 24% for HIP 13806.

The value of  $i$  is useful in indicating the most probable plane for planetary orbits, flagging possible planet occultation candidates (though errors on  $i$  make this a blunt tool), and giving the general orientation of the star (guiding first-guess positions for the location of active regions).

## 4. Modeling $v_r$ variation due to spots and plage

### 4.1. Simple estimates of $v_r$ variation due to spots

It is interesting first to compare our results with prediction from the models of Saar & Donahue (1997). The  $v_r$  amplitude ( $A_s$ ) due to a single spot goes as  $A_s \approx 6.5 f_s^{0.9} v \sin i$ , where  $f_s \approx 0.4 \Delta V$  if we assume spot latitude of 0°,  $\sin i = 1$ , and an average limb darkening coefficient of 0.6.  $\Delta V$  is the photometric amplitude in the V filter (here, we use the photometric amplitude in the Strömgren  $y$

filter as an approximate substitute). We list  $f_s$  and  $A_s$  in Table 4. Figure 3 shows our results for  $A_s$ , the predicted amplitude of  $v_r$  due to spottedness, versus the observed  $K$  velocity amplitude. Note that the  $A_s$  values are about a factor of two lower than  $K$  ( $\langle K/A_s \rangle = 2.0 \pm 0.3$ ). A very small part of this disagreement may come from the use of the  $y$  filter as opposed to the V filter, but we believe most of difference arises for two reasons. First, the Saar & Donahue (1997) spot models we used predict the maximum contribution  $v_r$  for a given  $f_s$  (due to a single, equatorial spot on a  $\sin i = 1$  star). Considering multiple spots with the same total  $f_s$  or a different  $\sin i$  (§3.2) will only reduce the predicted  $A_s$  further. However, the  $f_s$  values we used were *also* derived assuming single spots; thus the true  $f_s$  may be larger than Table 4 suggests. In the general case of multiple spots, one must model the full  $\Delta y$  and  $v_r$  curves. Beyond this, the presence of significant amounts of plage on our targets (as implied by, e.g., Ca II HK emission; (Radick et al. 1987)), indicates another possible source of  $v_r$  fluctuations. Thus, we must consider the possibility of multiple spots and plage contributing to the complex  $v_r$  curves.

Based on the above argument, in the case of multiple spots, relations connecting the rms *scatter* in  $\Delta y$  and  $v_r$  might be more useful than the amplitude. Although the data are still limited, there appears to be a trend between the rms scatter in  $\Delta y$  ( $\sigma_y$ ) and the rms  $v_r$  ( $\sigma_v$ ). Figure 4 shows  $\sigma_v$  versus  $\sigma_y$  of the observed data, including HD 166435, HD 19632 and HD 192263. A simple linear least squares fit yields  $\sigma_v[\text{m s}^{-1}] = 3600 \times \sigma_y + 2.29$ . Since when  $\sigma_y = 0$  this implies  $\sigma_v \approx 2.3 \text{ m s}^{-1} \approx \sigma_i$ , the internal error of the  $v_r$  data, the fit further supports the idea that much of the  $\sigma_v$  in these stars is due to spots.

#### 4.2. Modeling the $v_r$ effects of spots and plage

The effects of dark starspots on the measured  $v_r$  have been studied by Saar & Donahue (1997), Hatzes (1999), and Hatzes (2002). Plage, areas of relatively strong magnetic fields and activity which are optically bright, pose greater difficulties for modeling. Unlike spots, where the dominant effect is simply a strong reduction in the local continuum, in plage the alteration of normal convective motions by strong magnetic fields is not hidden from view by low surface brightness. To model the effects of plage we use the models presented in Saar (2003). Briefly, we use observed solar bisectors taken in plage and quiet regions at several limb angles as proxies for the bisectors of stellar intensity profiles,  $I_\nu$ . These proxies were then used to “warp” and shift symmetric  $I_\nu$  profiles computed in a simple Milne-Eddington model atmosphere. We then employed the now asymmetric quiet and plage  $I_\nu$ ’s to construct model stellar flux profiles for stars with any desired  $v \sin i$ , orientation, and plage geometry. Spots were modeled similarly, except that profiles inside spots were assumed to be symmetric. The centroid of the resulting profile was used to define  $v_r$  for the model.

We do not intend to present here a rigorous analysis of the spot and plage contributions to  $v_r$ ; this is left for a future paper. Our aim is only to (1) show that simple spot/plage models can explain details of the RV,  $y$  and H $\alpha$  variation beyond merely their amplitude and rms; and

(2) argue that it is thus *plausible* that spot and plage contribute significantly to the observed  $\Delta v_r$  variations. Our best fit solutions are not unique, and only indicative of a class of viable solutions under our chosen set of (hopefully physically reasonable) simplifying assumptions. Since the data are also taken over an extended period ( $\sim 4$  months), the best fit parameters necessarily represent time-averages of the related physical properties. This is not entirely unrealistic: active longitudes on active stars are known to persist for years (e.g., Jetsu 1996) and even solar active longitudes can be quite long-lived (Berdyugina & Usoskin 2003). Time averages therefore do have some relevant physical meaning. Since the plage models are based on solar line bisectors, we focused on the most solar-like of our Hyad targets, HD 26736.

Our assumptions are as follows. The most significant one is that the spot/plage reside at latitudes  $\theta = 30^\circ$  (near the subobserver  $\theta \approx 20^\circ$  for HD 26736), which yields close to the maximum effect for a given region area. We adopt a spot temperature of  $T_s = 4000$  K (similar to the Sun), corresponding to a fractional continuum difference in spots at  $5000\text{\AA}$  (relative to the quiet photosphere) of  $\Delta I_S = (I_Q - I_S)/I_Q = -90\%$ . Additionally, for simplicity, we took the fractional continuum difference in plage (also relative to the quiet photosphere), to be  $\Delta I_P = (I_Q - I_P)/I_Q = 0$ . A linear limb-darkening coefficient  $\epsilon = 0.6$  was adopted, and the regions were assumed circular.

We first attempted to model the observed  $\Delta y$  from HD 26736, successively adding features of varying radius and longitude to fit  $\Delta y$ . Since we have adopted  $\Delta I_P = 0$ , spots must completely account for the observed  $\Delta y$ . We then apply the resulting spot sizes and positions to compute a model for spot-induced  $v_r$  variation. By not *fitting*  $v_r$ , but rather letting the observed  $\Delta y$  drive the modeling, we ensure that the resulting  $v_r$  model is consistent with  $\Delta y$  but does not attempt to “explain” features which are not due to spots. For our assumed  $\theta$ , a single spot spans only a phase range  $\delta\phi \approx 0.5$  (Fig. 5a) and thus cannot alone describe the photometry. The  $\Delta y$  variation could be reasonably well described with two features (see Table 5 for their properties; fit RMS  $\sigma_{\text{fit}}(y) = 0.00394$ ) We find an optimum “background” unmodulated brightness of  $\Delta y = 0.988$  (due to the pristine photosphere plus any uniform spot component). The resulting  $v_r$  model agrees fairly well for  $\phi > 0.85$  and  $\phi < 0.4$ , but there are some discrepancies elsewhere. The discrepancies are strongest around phase  $\phi = 0.75$ , where the differences between  $v_r$  and the spot-only model are  $\approx 50 \text{ m s}^{-1}$ . Adding a third spot could partly correct this, only to introduce new fitting errors to  $v_r$  around  $\phi = 0.9$ , and errors in  $\Delta y$  near  $\phi = 0.6$ .

The remaining systematic differences between the spot-only model and  $v_r$  could be due to plage, our assumptions (especially the restriction on  $\theta$ ), or even potentially a planet. To investigate the first possibility, it is useful to have a plage diagnostic analogous to  $\Delta y$ . As our HET spectra do not contain the traditional plage indicator Ca II H & K, we constructed a substitute from the H $\alpha$  profile as follows. First, telluric features were removed by ratioing the HD 26736 data with a scaled spectrum of a rapidly rotating A star, whose broad H $\alpha$  feature was removed with a cubic spline fit. The average flux in a  $2.15\text{\AA}$  interval centered on the H $\alpha$  core was then ratioed with the average flux in a nearby, nearly line-free “continuum” segment ( $5\text{\AA}$  centered at  $6602\text{\AA}$ ) to form an H $\alpha$  index  $S_{\text{H}\alpha} = F_{\text{H}\alpha\text{core}}/F_{\text{con}}$ . This index showed a small but significant modulation at  $P_v$



(Fig. 5b). Comparison of Figs. 5a and 5b reveals that the plage emission areas are not coincident with the spots: the  $S_{\text{H}\alpha}$  curve maximum is shifted from the  $\Delta y$  minimum, and there are features in  $S_{\text{H}\alpha}$  not obvious in  $\Delta y$  (e.g., the enhancement near  $\phi \approx 0.9$ ).

Next, in a fashion similar to the spot-modeling we added plage regions until the the  $S_{\text{H}\alpha}$  data was reasonably well fit. We assumed that the  $\text{H}\alpha$  emission is limb-brightened with  $\epsilon = -0.2$ . An estimate for the intrinsic plage emission strength per unit area,  $I_{S(\text{H}\alpha)}$ , was also needed. There has been relatively little work using  $\text{H}\alpha$  as an activity diagnostic in low-to-moderate activity G and K stars. Herbig (1985) found the minimum flux for an early G star in a  $1.7\text{\AA}$  bandpass under the  $\text{H}\alpha$  core (expressed as an equivalent width) is  $W_\lambda \approx 0.74 \text{\AA}$ . His most active target,  $\xi \text{ UMa B}$  (G5V,  $P_{\text{rot}} = 3.98\text{d}$ ) observed with a slightly different bandpass, showed  $\Delta W_\lambda \approx 0.277 \text{\AA}$  above this baseline level. If we assume the latter represents a “saturated” chromosphere star ( $f_p \approx 1$ ) and the former a completely inactive star ( $f_p \approx 0$ ), we find (after correcting for resolution and bandpass differences)  $I_{S(\text{H}\alpha)} \approx 0.016$  for a plage at disk center with an area of 10% of the visible surface. With these assumptions we found good fits came for a “background”  $S_{\text{H}\alpha} = 0.475$  (due to the photospheric  $\text{H}\alpha$  and any uniform plage/network component). We note, however, that there is a trade-off between plage brightness and area, i.e., fits to  $S_{\text{H}\alpha}$  are equivalent for  $I_{S(\text{H}\alpha)} \times \Sigma f_p \approx \text{constant}$ . Thus, changes in  $I_{S(\text{H}\alpha)}$  affects plage areas and thereby the plage contribution to  $v_r$ . A minimum of 3 regions were required (see Table 5;  $\sigma_{\text{fit}}(S_{\text{H}\alpha}) = 0.00219$ ); the positions of the model spots and plage are also indicated in Fig. 5. The resulting plage-induced  $\Delta v_r$  ends up being rather small relative to the spot contribution (model amplitudes of  $A_P \approx 16 \text{ m s}^{-1}$  compared with  $A_S \approx 83 \text{ m s}^{-1}$ ; Fig. 5d). The inclusion of the plages (at  $\theta = 30^\circ$ ) does not significantly alter the agreement between the resulting  $v_r$  model and the data: the RMS between them is  $\sigma = 29.1 \text{ m s}^{-1}$ . Including plage makes the agreement slightly worse around  $\phi \approx 0.1 - 0.3$  by the plage, but slightly better near  $\phi \approx 0.5 - 0.7$ ; significant discrepancies remain (Fig. 5d). Whether these discrepancies show any systematic trends (suggesting a possible underlying planetary signal) must await more rigorous modeling, in particular relaxing the assumption of  $\theta = 30^\circ$  for all regions. We leave this for a future paper.

## 5. Discussion and Conclusions

This initial search for short-period planets in the Keck Hyades survey has instead turned up several lines of evidence pointing to  $v_r$  variations driven by magnetic activity. First, the photometric and the  $v_r$  variations show similar periodicities (Fig. 1; Table 1); the one star studied here in  $\text{H}\alpha$  (HD 26736) shows a similar periodicity in that activity diagnostic as well (Fig. 5b). The  $v_r$  amplitudes increase with the  $\Delta y$  photometric amplitudes in a way consistent with (though smaller than) predictions of a simple single-spot model (Saar & Donahue 1997, Fig. 3). The rms scatter in  $\Delta y$  and  $v_r$  also show a linear relationship (Fig. 4). This correlation is potentially quite useful as a simple way of estimating  $\sigma_v$  from photometry. More data must be collected before we can predict  $\sigma_v$  from  $\sigma_y$  with confidence; the relationship may depend on other properties/parameters.

Once refined, though, such a correlation may be of use to rapidly help flag “problem” stars which will require more careful analysis to confirm planets, to screen out such stars from search lists, or to estimate what fraction of a given star’s  $\sigma_v$  is likely due to activity.

The phase shifts between the  $v_r$  and  $\Delta y$  curves clearly seen in at least two of the stars (HIP 13806 and HD 26736) are also consistent with a spot origin for much of the  $v_r$  variation. To see this, consider that the perturbation from a single, black spot at  $\theta = 0$  on a star (with  $i = 90^\circ$  and no limb-darkening) scales as  $\Delta v_r \propto -f_s \sin \phi \cos \phi$  (where  $\phi$  is the phase angle measured from the sub-observer meridian  $\phi = 0$ ) while photometry varies as  $\Delta y \propto f_s \cos \phi$ . The minimum light (at  $\phi = 0$ ) is shifted from the maximum  $\Delta v_r$  (at  $\phi = -45^\circ$ ); the actual shift will depend on details of the limb-darkening and active region geometry. HIP 13806 and HD 26736 (Fig. 1) both show this pattern of  $v_r$  maxima preceding light minima. The case of HD 26767 is less clear (two  $v_r$  near  $\phi \approx 0.4$  are discrepant), but if one identifies the primary maximum with the feature near  $\phi \approx 0.2$ , it also follows the pattern. Queloz et al. (2001) also see this phase shift in HD 166435.

Finally, beyond these more qualitative connections of  $v_r$  with spots and plage, we have also demonstrated that the  $v_r$  variations can be modeled directly. By first modeling the observed photometry and H $\alpha$  emission and using the inferred spot and plage locations and sizes in simple models of these regions’  $v_r$  properties, we can explain a significant fraction of the  $v_r$  variation of vB 15 in detail (Fig. 5). Given internal errors of  $\sigma_i(y) \approx 0.003$  (the constancy of the comparison stars) and  $\sigma_i(S_{H\alpha}) \approx 0.0025$ , our fits to  $\Delta y$  and  $S_{H\alpha}$  are reasonably successful with two spots and three plages, respectively ( $\chi^2_\nu = 1.7$  and  $\chi^2_\nu = 0.8$ ). The resulting  $v_r$  models are less successful in explaining all the velocity variations ( $\sigma \approx 29 \text{ m s}^{-1}$ ;  $\chi^2_\nu \approx 26$ ) but is able to account for  $\approx 50\%$  of the variance in the  $v_r$  data. Some of the discrepancies are undoubtedly due to our simplifying assumptions, such as all regions placed at  $\theta = 30^\circ$ . Some less obvious implicit assumptions (e.g., that all spots and all plages are identical in how they act on  $v_r$ , that the solar plage bisectors used as proxies are representative of stellar plage) may also be important. Still, despite the fact that the modeling presented here is simplified and certainly not definitive, we believe that it argues that a combination of spot and plage can explain many of the  $v_r$  fluctuations seen in HD 26736. By analogy, we suspect that many of the  $v_r$  variation seen in the other targets can be similarly explained by activity. Indeed, the  $v_r$  “jitter” in HD 26756 without corresponding  $\Delta y$  changes or strong periodicity might be the result of rapidly evolving plage dominating the  $v_r$  perturbations.

Young stars present distinct problems for the search for short-period planets. Our work shows that photometric confirmation along with good activity measurements are a very helpful check to insure the viability of short-period planetary candidates. It is important to note that active stars need not necessarily be excluded from planet searches since it should be possible (at least in principle) to remove activity-related perturbations from  $v_r$  measurements. Saar & Fischer (2000) show that simple correlations between  $v_r$  and a plage diagnostic (e.g., H $\alpha$ , Ca II H & K) can be effective in removing long-timescale variations in  $v_r$  stemming, for example, from magnetic cycle variations in mean plage area. On shorter (rotational) timescales, this might be accomplished

by modeling the activity features (as explored here) or by monitoring line shape changes (e.g., bisectors) as indicators of rotating inhomogeneous features (Saar et al. 2001; Saar et al. 2002; Queloz et al. 2001).

Magnetic activity and hence activity-induced  $v_r$  variations will occur on a wide range of timescales (see for example, Fig. 11 from Jenkins (2002) showing solar photometric variability extrapolated to stars; also, Donahue et al. (1997a,b) for stellar Ca II HK variability). It is important to note, however, that most of the strongly *periodic* power will be concentrated on distinct surface/activity timescales:  $P_{\text{rot}}$ , differential rotation, active region growth/decay, active longitude growth/decay (including “flip-flops”; see e.g., Jetsu, Pelt, & Tuominen 1993), and magnetic cycle. Planets with orbital periods well separated from these timescales will be much easier to detect and confirm.

The models also indicate the possibility that plage-induced  $v_r$  fluctuations without strong, parallel photometric variations must also be considered as possible contributors to  $v_r$  signals. Since plage-to-spot area ratios are largest on inactive stars, it is quite possible that plage-induced  $\Delta v_r$  may dominate on these objects.

Quite apart from planet searches, our work suggests the possible use of precision  $v_r$  measurements to investigate surface features on cool stars. The  $v_r$  variation as a function of rotational phase is distinctly different for spots and plage, and shows significantly sharper changes with  $\phi$  than photometry or chromospheric activity (Fig. 5c). This makes high precision  $v_r$  curves a powerful tool for investigating stellar surface structures, and one uniquely suited for the study of plages and slower rotators ( $v \sin i \lesssim 12 \text{ km s}^{-1}$ ), for which Doppler imaging is less useful.

DBP and WDC are supported by NASA grant NAG5-9227 and NSF grant AST-9808980. SHS was supported by NASA Origins program grant NAG5-10630. GWH acknowledges support from NASA grants NCC5-96 and NCC5-511 as well as NSF grant HRD-9706268. We would like to thank Artie Hatzes and Chris Sneden for many useful discussions and Rob Robinson and Frank Bash for making the time critical observations at HET possible.

## REFERENCES

- Allende Prieto, C. & Lambert, D. L. 1999, A&A, 352, 555
- Berdyugina, S. V. & Usoskin, I. G. 2003, A&A, 405, 1121
- Castelli, F., Gratton, R. G., & Kurucz, R. L. 1997, A&A, 318, 841
- Cochran, W. D., Hatzes, A. P., Butler, R. P., & Marcy, G. W. 1997, ApJ, 483, 457
- Cochran, W. D., Hatzes, A. P., & Paulson, D. B. 2002, AJ, 124, 565

- Cochran, W. D., Tull, R. G., MacQueen, P. J., Paulson, D. B., & Endl, M. 2003, in *Scientific Frontiers in Research on Extrasolar Planets*, ASP Conference Series, ed. D. Deming, in press
- Donahue, R. A., Dobson, A. K., & Baliunas, S. L. 1997a, *Sol. Phys.*, 171, 191
- . 1997b, *Sol. Phys.*, 211
- ESA. 1997, *The Hipparcos and Tycho Catalogues* ESA SP-1200
- Gray, D. F. 1992, *The Observation and Analysis of Stellar Photospheres* (Cambridge: Cambridge University Press)
- Hatzes, A. P. 1999, in *ASP Conf. Ser. 185: IAU Colloq. 170: Precise Stellar Radial Velocities*, 259
- Hatzes, A. P. 2002, *Astronomische Nachrichten*, 323, 392
- Hatzes, A. P., Cochran, W. D., McArthur, B., Baliunas, S. L., Walker, G. A. H., Campbell, B., Irwin, A. W., Yang, S., Kürster, M., Endl, M., Els, S., Butler, R. P., & Marcy, G. W. 2000, *ApJ*, 544, L145
- Henry, G. W. 1999, *PASP*, 111, 845
- Henry, G. W., Donahue, R. A., & Baliunas, S. L. 2002, *ApJ*, 577
- Henry, G. W., Fekel, F. C., Kaye, A. B., & Kaul, A. 2001, *AJ*, 122, 3383
- Herbig, G. H. 1985, *ApJ*, 289, 269
- Horne, J. H. & Baliunas, S. L. 1986, *ApJ*, 302, 757
- Jenkins, J. M. 2002, *ApJ*, 575, 493
- Jetsu, L. 1996, *A&A*, 314, 153
- Jetsu, L., Pelt, J., & Tuominen, I. 1993, *A&A*, 278, 449
- Kurucz, R. L., Furenlid, I., & Brault, J. 1984, *Solar flux atlas from 296 to 1300 NM* (National Solar Observatory Atlas, Sunspot, New Mexico: National Solar Observatory, 1984)
- Mayor, M. & Queloz, D. 1995, *Nature*, 378, 355
- Paulson, D. B., Saar, S. H., Cochran, W. D., & Hatzes, A. P. 2002, *AJ*, 124, 572
- Paulson, D. B., Sneden, C., & Cochran, W. D. 2003, *AJ*, in press
- Queloz, D., Henry, G. W., Sivan, J. P., Baliunas, S. L., Beuzit, J. L., Donahue, R. A., Mayor, M., Naef, D., Perrier, C., & Udry, S. 2001, *A&A*, 379, 279

- Radick, R. R., Thompson, D. T., Lockwood, G. W., Duncan, D. K., & Baggett, W. E. 1987, *ApJ*, 321, 459
- Saar, S. 2003, in *Scientific Frontiers in Research on Extrasolar Planets*, ASP Conference Series, ed. D. Deming, in press
- Saar, S. & Osten, R. 1997, *MNRAS*, 284, 284
- Saar, S. H., Butler, R. P., & Marcy, G. W. 1998, *ApJ*, 498, L153, =SBM
- Saar, S. H. & Donahue, R. A. 1997, *ApJ*, 485, 319
- Saar, S. H. & Fischer, D. 2000, *ApJ*, 534, L105
- Saar, S. H., Fischer, D., Snyder, N., & Smolec, R. 2001, in *Cool Stars, Stellar Systems and the Sun 11*, ASP Conf. Series, Vol. 223, CD-1051
- Saar, S. H., Hatzes, A. P., Cochran, W. D., & Paulson, D. B. 2002, in *Cool Stars, Stellar Systems and the Sun 12*, University of Colorado Press, in press
- Santos, N. C., Mayor, M., Naef, D., Pepe, F., Queloz, D., Udry, S., & Blecha, A. 2000, *A&A*, 361, 265
- Snedden, C., Kraft, R. P., Prosser, C. F., & Langer, G. E. 1991, *AJ*, 102, 2001
- Snedden, C. A. 1973, Ph.D. Thesis
- Toner, C. G. & Gray, D. F. 1988, *ApJ*, 334, 1008
- Tull, R. G. 1998, *Proc. Soc. Photo-opt. Inst. Eng.*, 3355, 387
- Vogt, S. S., Penrod, D., & Hatzes, A. P. 1987, *ApJ*, 321, 496

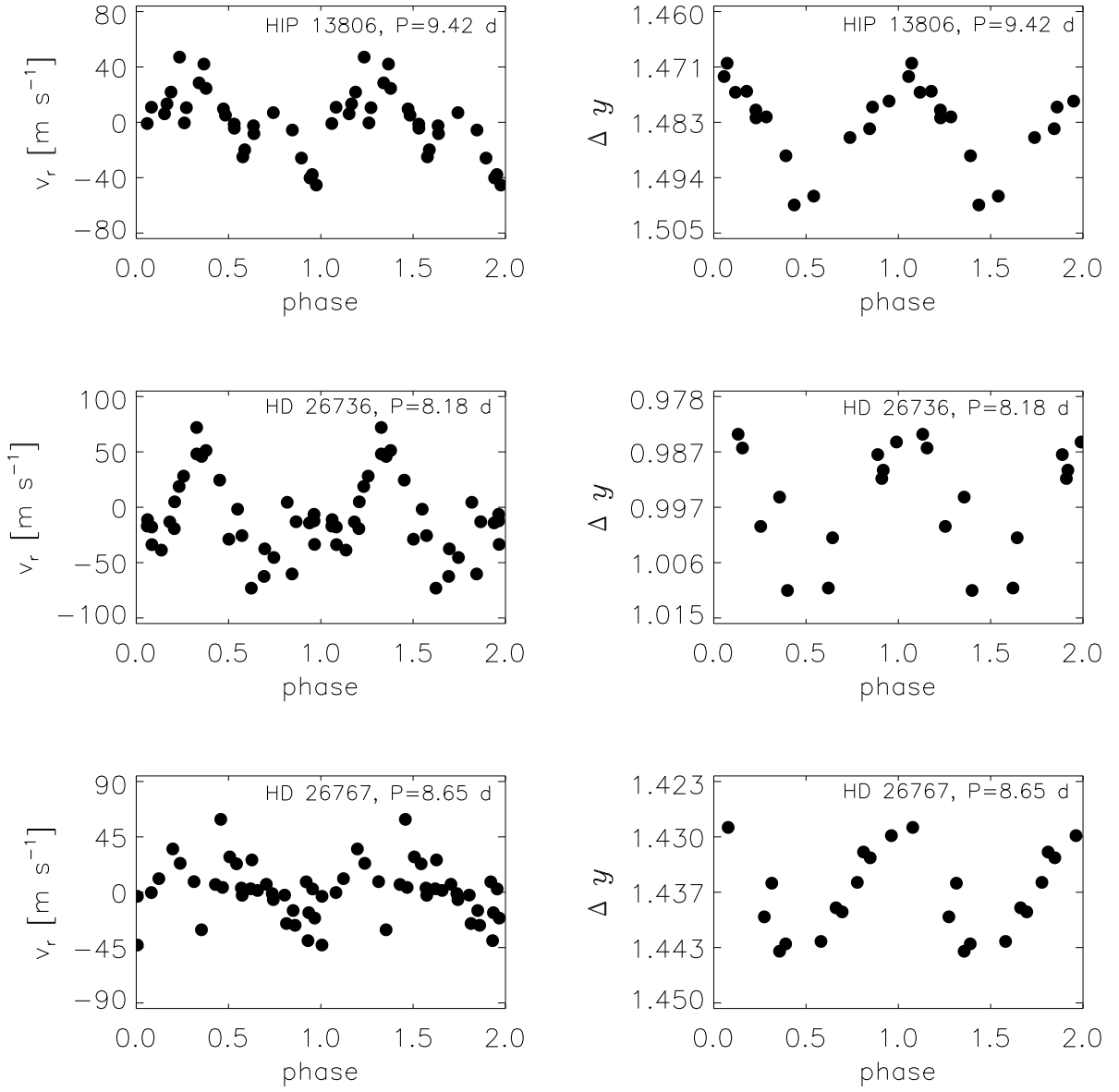


Fig. 1.— Program stars:  $v_r$  (left) and differential Strömgren  $y$  (right) curves.

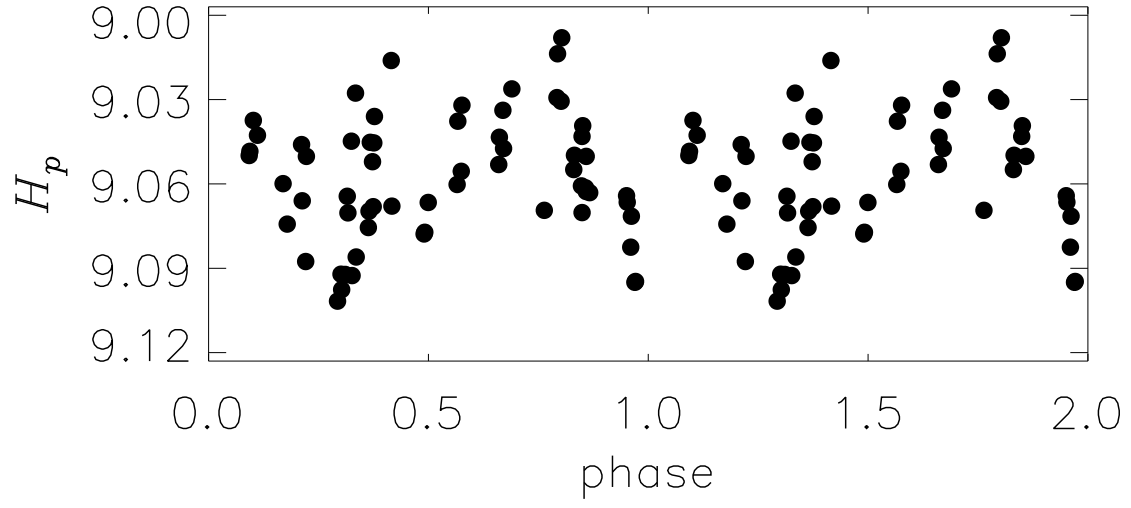


Fig. 2.— Hipparcos photometric data ( $H_p$ ) for HIP 13806, phased to 9.42 days.

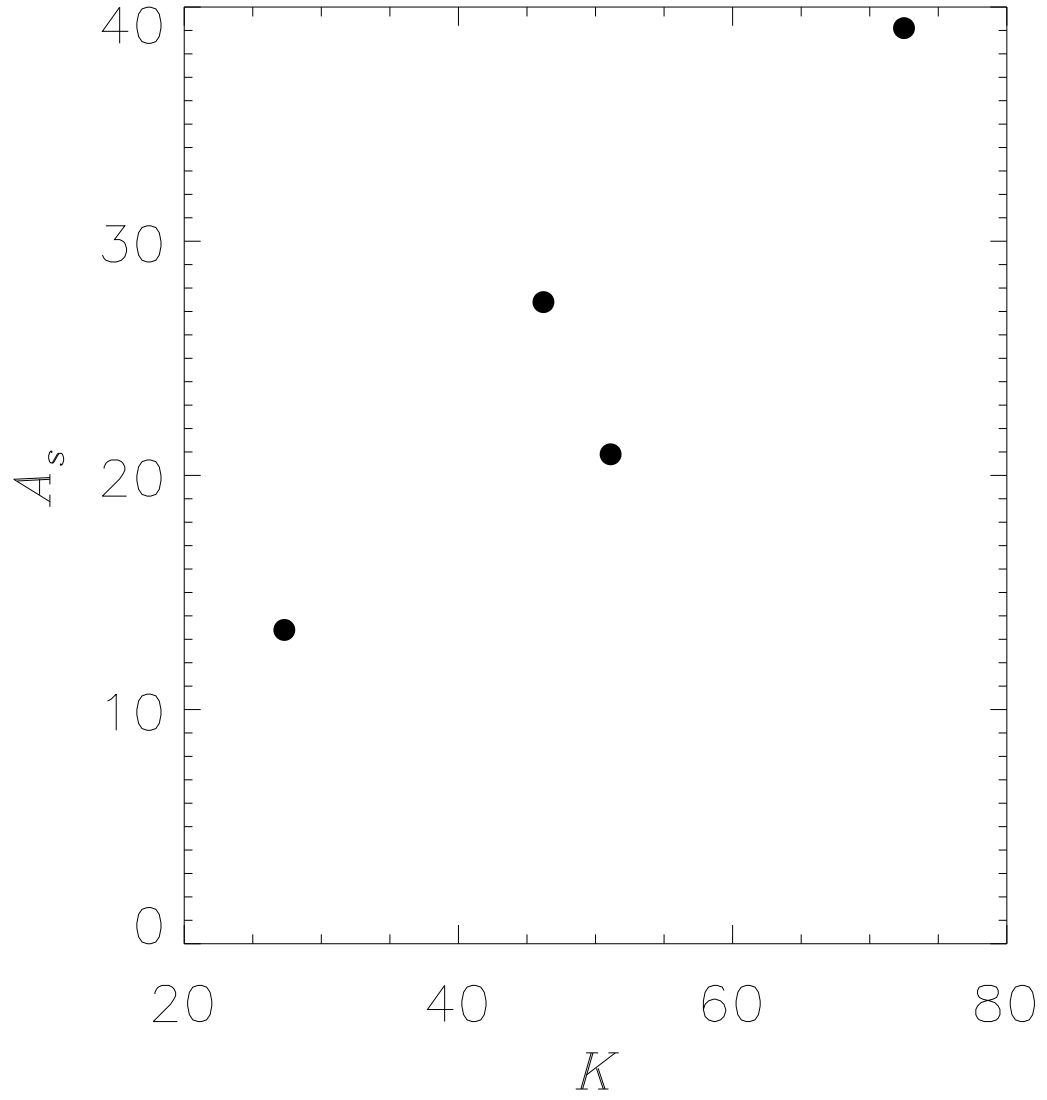


Fig. 3.—  $v_r$  amplitude,  $A_s$ , as predicted from Saar & Donahue (1997) versus  $K$  for our program stars.



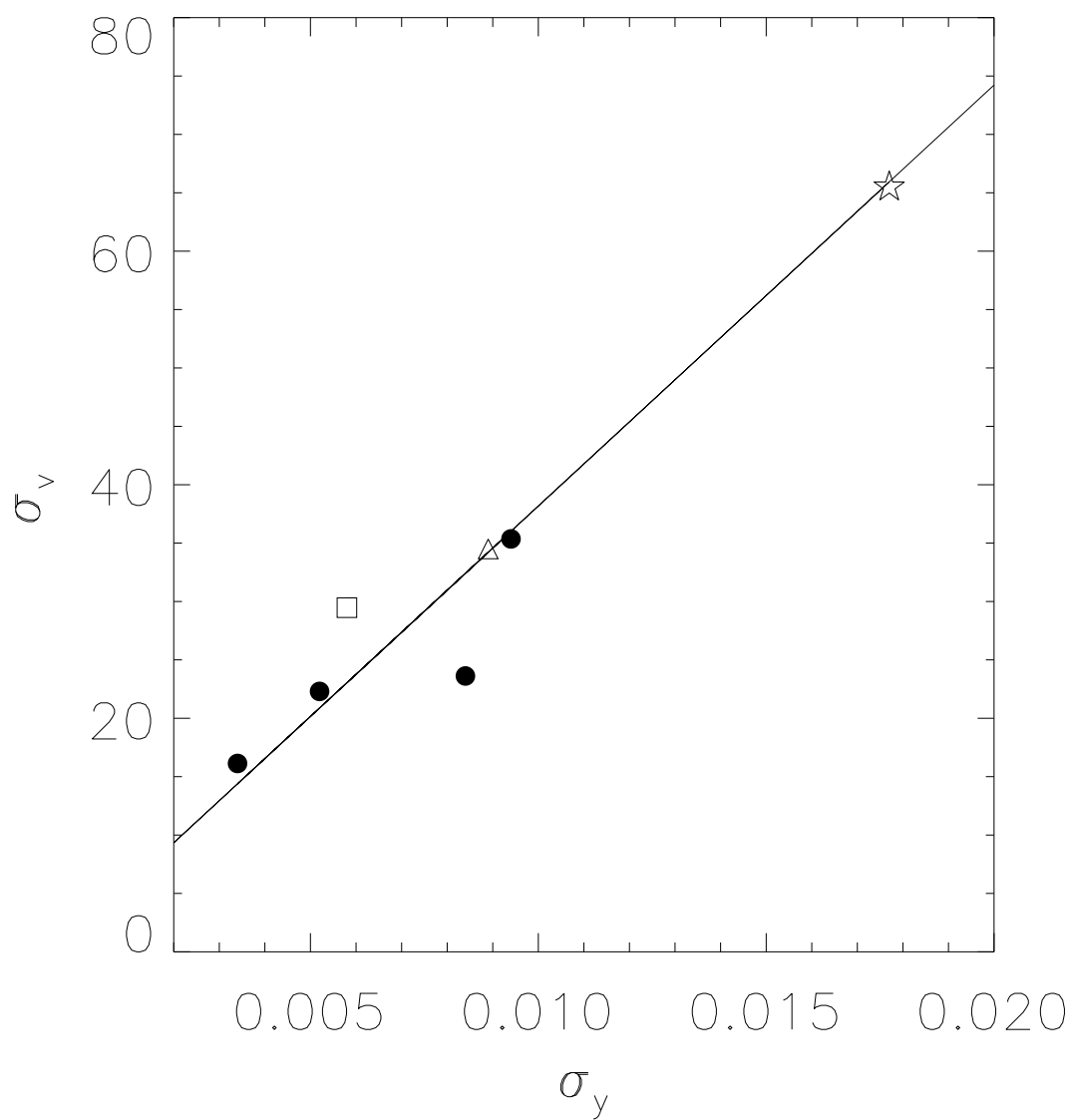


Fig. 4.—  $v_r$  rms versus  $y$  rms for our program stars (*circles*), HD 166435 (Queloz et al. 2001) (*star*), HD 19632 (private communication, G. Henry, P. Butler 2002) (*box*) and HD 192263 (Henry et al. 2002) (*triangle*).

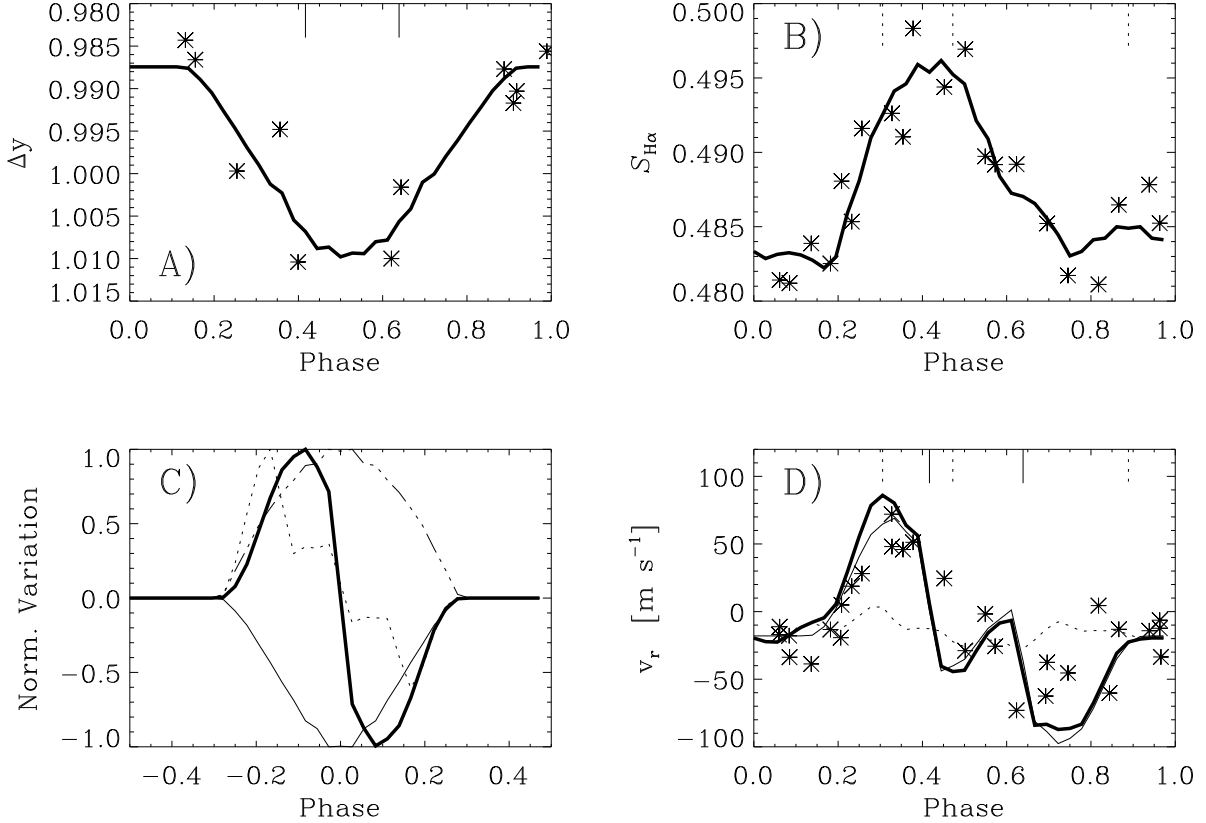


Fig. 5.— Observed  $\Delta y$ ,  $S_{H\alpha}$ , and  $v_r$  for HD 26736 plus models (see Table 5 for model parameters, text for details). A) Observed  $\Delta y$  (stars), best-fit two spot model for  $\Delta y$  (solid;  $\sigma_{\text{fit}} = 0.00394$ ), with phase of model spot meridian passage marked (vertical ticks). B)  $S_{H\alpha}$  computed from observed  $H\alpha$  profiles (stars), best-fit 3 plage model for  $S_{H\alpha}$  (solid;  $\sigma_{\text{fit}} = 0.00219$ ), with phase of plage meridian passage marked (vertical ticks). C) Normalized variation for a single spot  $v_r$  (heavy solid),  $\Delta y$  (solid), single plage  $v_r$  (heavy dashed), and  $S_{H\alpha}$  (dashed). Maximum amplitudes are  $25.5 \text{ m s}^{-1}$  and  $0.0112 \text{ mag}$  for a  $f_S=1\%$  spot, and  $3.0 \text{ m s}^{-1}$  and  $0.0128 \text{ H}\alpha$  units for a  $f_P=1\%$  plage. D) Observed  $v_r$  (stars),  $v_r$  of the two spot model which best fits  $\Delta y$  in panel A (solid;  $\sigma = 29.0 \text{ m s}^{-1}$ ),  $v_r$  of the 3 plage model which best fits  $S_{H\alpha}$  in panel B (dotted), and the  $v_r$  of the combined spot + plage model (heavy solid;  $\sigma = 29.1 \text{ m s}^{-1}$ ). Vertical ticks (top) mark phase of central meridian passage of model spots (solid) and plages (dashed).

Table 1. Program Information

Star	vB#	# $v_r$ obs.	K [m s <sup>-1</sup> ]	$P_{rot,v_r}$ [days]	FAP $_{v_r}$ [%]	# phot. obs.	$\Delta y$	$P_{rot,phot}$ [days]	FAP $_y$ [%]	# Hipp. obs.	$P_{rot,Hipp.}$ [days]	FAP <sub>HIP</sub> [%]
HIP 13806	153	25	46.2	9.42	1.7	14	0.028	9.18	4.3	62	9.60	0.02
HD 26767	18	30	51.1	8.65	7.9	12	0.015	8.65	5.9	34	...	...
HD 26736	15	29	72.5	8.18	1.4	11	0.026	8.44	15.5	102	...	...
HD 26756	17	24	27.3	...	...	12	0.011	...	...	44	...	...

Table 2. Radial Velocities

Star	JD - 2400000	$v_r$ [m s <sup>-1</sup> ]	Uncertainty [m s <sup>-1</sup> ]
HIP 13806	52262.770111	27.11	6.35
	52263.768303	8.46	5.56
	52265.558250	-21.27	6.61
	52266.564679	-28.23	6.80
	52269.747800	-65.33	18.06
	52270.756446	-9.11	6.52
	52271.754419	1.83	8.31
	52297.687220	-60.20	4.61
	52299.682102	-13.88	4.89
	52300.694922	-20.44	4.46
	52301.692142	22.06	7.63
	52302.690889	-10.32	3.82
	52303.678815	-44.98	4.75
	52306.669150	-45.84	3.63
	52312.664745	-24.29	7.08
	52313.641222	-22.49	3.22
	52314.656157	-13.03	16.02
	52315.627230	-25.59	5.16
	52316.642697	-57.75	4.17
	52317.638826	-20.89	5.27
	52318.648681	-6.70	5.12
	52319.639116	-9.43	5.11
	52320.642096	4.52	5.29
	52321.632011	-14.87	5.60
	52322.615422	-39.87	3.69
HD 26767	52199.811224	59.23	5.84
	52200.812501	-2.48	5.58
	52202.803337	-2.36	4.92
	52203.814494	8.44	6.58
	52236.872727	-6.04	7.40
	52237.893749	-26.90	6.69
	52252.676137	3.40	9.22
	52253.845854	6.45	5.58
	52255.835060	-16.65	5.01
	52261.818689	26.24	7.64
	52299.701994	-42.94	5.98
	52300.710344	11.01	4.25
	52301.708195	23.47	4.49
	52302.706162	-30.54	4.56
	52303.693759	3.89	3.78
	52306.688347	-25.46	4.00
	52307.697467	-39.37	4.80
	52312.681499	28.70	4.82
	52313.660480	2.78	4.51
	52314.671760	-1.10	4.39
	52315.651757	-14.89	4.96
	52316.661289	-21.04	4.07
	52317.656991	-0.28	5.26
	52318.663084	35.16	4.12

Table 2—Continued

Star	JD - 2400000	$v_r$ [m s <sup>-1</sup> ]	Uncertainty [m s <sup>-1</sup> ]
HD 26736	52319.657755	8.61	4.17
	52320.659775	6.29	4.30
	52321.649747	23.07	4.23
	52322.634036	1.43	4.13
	52325.654987	-3.34	4.86
	52238.711713	2.63	5.79
	52263.619768	-12.31	7.38
	52264.606026	-17.85	5.86
	52265.606621	-19.30	6.01
	52266.597528	72.02	6.38
	52269.584370	-62.45	7.75
	52270.823349	-60.25	7.72
	52271.821446	-33.54	7.08
	52272.587749	-16.98	6.58
	52297.754247	-38.71	6.04
	52298.738493	28.13	4.79
	52299.731856	51.27	5.45
	52300.743482	-28.87	6.69
	52301.739367	-73.07	9.49
	52302.737520	-45.38	5.23
	52303.724341	-13.08	4.96
	52306.719880	18.78	5.27
	52307.715564	45.90	4.02
	52312.698359	-6.38	4.56
	52313.693807	-33.77	3.38
	52314.702460	4.90	4.38
	52315.681787	48.11	5.03
	52316.697637	24.51	4.73
	52317.684034	-25.61	4.63
	52318.693958	-37.56	5.22
	52319.690237	4.46	4.76
	52320.675927	-14.14	4.64
	52321.680885	-11.19	6.62
	52322.667651	-13.24	5.56
	52325.671298	-1.74	4.41
HD 26756	52200.796965	-11.69	6.23
	52202.783532	25.82	6.74
	52203.989956	16.65	7.52
	52247.879099	13.27	8.14
	52249.861960	-19.19	6.70
	52252.660236	-8.91	8.12
	52253.861596	-7.63	7.69
	52255.851520	-5.29	6.40
	52278.591680	16.13	8.26
	52299.717028	10.40	5.72
	52300.725215	-28.88	5.29
	52301.721528	-18.92	5.71
	52302.719726	-17.26	4.65
	52303.709706	2.60	5.18

Table 2—Continued

Star	JD - 2400000	$v_r$ [m s <sup>-1</sup> ]	Uncertainty [m s <sup>-1</sup> ]
	52306.703796	-26.66	4.96
	52313.677015	15.59	4.35
	52314.685147	-13.61	5.33
	52315.666452	3.35	4.85
	52316.679270	-1.12	5.27
	52317.670296	-16.98	5.36
	52318.677153	0.27	5.77
	52319.673016	16.77	5.08
	52321.664983	25.44	5.34
	52322.651275	-1.53	5.26

Table 3. Photometry

Star	JD - 2400000	$\Delta y$
HIP 13806	52314.6093	1.4856
	52315.6109	1.4838
	52316.6031	1.4782
	52317.6049	1.4732
	52327.6049	1.4764
	52328.6443	1.4800
	52328.6548	1.4816
	52330.6054	1.4993
	52331.5996	1.4975
	52334.5989	1.4794
	52336.5999	1.4705
	52337.5993	1.4762
	52338.5994	1.4814
	52339.5992	1.4893
HD 26767	52315.6295	1.4323
	52316.6226	1.4296
	52317.6234	1.4286
	52328.6820	1.4437
	52330.6221	1.4425
	52331.6163	1.4389
	52332.6166	1.4316
	52336.6171	1.4395
	52337.6166	1.4428
	52345.6180	1.4354
HD 26736	52348.6278	1.4384
	52349.6254	1.4353
	52328.6250	0.9917
	52328.6897	0.9903
	52330.6308	0.9866
	52332.6253	1.0104
	52334.6239	1.0016
	52336.6245	0.9877
	52338.6183	0.9843
	52339.6184	0.9997
HD 26756	52342.6175	1.0100
	52345.6350	0.9856
	52348.6352	0.9948
	52315.6295	1.8513
	52316.6226	1.8556
	52317.6234	1.8442
	52328.6820	1.8514
	52330.6221	1.8531
	52331.6163	1.8516
	52332.6166	1.8533
	52336.6171	1.8450
	52337.6166	1.8531
	52345.6180	1.8487
	52348.6278	1.8495
	52349.6254	1.8502

Table 3—Continued

Star	JD - 2400000	$\Delta y$
------	--------------	------------



Table 4. Stellar Parameters

Star	vB #	$T_{\text{eff}}$ [K]	$\log g$	$\xi$ [km s <sup>-1</sup> ]	[Fe/H]	$\zeta$ [km s <sup>-1</sup> ]	$v \sin i$ [km s <sup>-1</sup> ]	$\sin i$	$f_s$ [%]	$A_s$ [m s <sup>-1</sup> ]
HIP 13806	vB 153	5150	4.5	0.60	0.19	2.3	3.8	0.91	1.10	27
HD 26767	vB 18	5900	4.4	0.80	0.23	3.9	5.4	0.83	0.60	21
HD 26736	vB 15	5750	4.4	0.80	0.19	3.8	5.4	0.94	1.00	39
HD 26756	vB 17	5650	4.4	0.80	0.17	3.5	4.5	...	0.44	13

Table 5. Spot and Plage Parameters: HD 26736

Region	$\phi_0$	Area [%]
spot 1	0.42	1.15
spot 2	0.64	1.05
plage 1	0.31	1.15
plage 2	0.47	2.30
plage 3	0.89	1.30